Oxygen distribution in $YBa_2Cu_3O_{7-x}$ single crystals with $x > 0.5$

Yu. A. Barabanenkov, N. D. Zakharov, B. Ya. Kotyuzhanskiy, V. A. Meleshina,
L. E. Svistov, and A. Ya. Shapiro

Shubnikov Institute of Crystallography, USSR Academy of Sciences

The structure of $YBa_2Cu_3O_{7-x}$ high-temperature superconducting single crystals with an average oxygen concentration corresponding to $x = 0.7$ is investigated by transmission electron microscopy. It is demonstrated that this compound is characterized by an inhomogeneous oxygen distribution throughout the crystal: The specimen is divided into blocks with different oxygen concentrations. The oxygen concentration varies from block to block over the interval $0.5 \leqslant x \leqslant 1$. The characteristic block size is $\sim 100 \times 10 \times 20$ nm^3. Annealing at $T = 370$ °C accompanied by diffusion of the oxygen over a distance substantially exceeding the block size could not eliminate the nonuniform oxygen distribution.

As early as the initial studies[1-8] identifying the significant influence of oxygen concentration on the structure and physical properties of the high-temperature superconducting compound $YBa_2Cu_3O_{7-x}$ substantial attention has been devoted to both an analysis of this phenomenon and methods of fabricating specimens with different oxygen concentrations (see, for example, Refs. 9, 10 and the references cited therein) and studies of the mechanisms behind oxygen ion distribution in the crystalline lattice on the micro- and macroscopic scales (Refs. 1, 11–22, etc.). However a great deal has remained unclear to date on these issues. This is especially true of crystals with $x \geqslant 0.5$. Specifically it has not yet been determined whether or not monophase specimens exist with an oxygen concentration in the interval corresponding to $0.5 < x < 1$ or, as has been claimed by, for example, Ref. 20, the oxygen in crystals with such an average oxygen concentration is nonuniformly distributed and such crystals consist of rhombic structural blocks with $x = 0.5$ and tetragonal ones with $x = 1$. If the latter is true the wide variation in electrical and other properties observed by other authors in specimens with a low oxygen concentration (see, for example, Ref. 1, 23–26) becomes clear.

The present paper attempts to investigate the oxygen distribution in $YBa_2Cu_3O_{6.3}$ single crystals for which the structure of matter in various regions of the specimens was analyzed by means of transmission electron microscopy. Single crystals with such an average oxygen concentration ($x \approx 0.7$) were fabricated by the growing technique described in Ref. 27 which includes in the last stage of the process rapid air cooling from $T_q \sim 900$ °C near the melting point of the initial blend. No substantial variation in the overall oxygen concentration in the specimens was identified in the subsequent experiments.

The test specimens were thin single crystal wafers of characteristic dimensions $1 \times 1 \times 0.03$ mm^3 with (001) basal faces. The average oxygen concentration x in the specimen was determined to within $\Delta x = \pm 0.05$ from the unit cell parameter c using the data from Ref. 1. The parameter c was measured by an x-ray single-crystal diffractometer at the Bragg peak (006) $\sim 6'$ in width.

The specimens were reduced by ionic etching to ~ 10 nm in order to obtain a high-resolution electron microscopy image (an HREM-image). There was no appreciable heating of the specimen by ion or electron beams during the etching process or during the measurements (it was estimated to be less than ~ 100 °C). The possibility of a variation in the structure of the specimen observed from the HREM-image due to the effects outlined above can be eliminated for the following reasons. First, according to Ref. 10, which investigated oxygen saturation of the test compound, oxygen depletion of only 1–2 atomic layers near the crystal surface will occur during the experiment in a vacuum at $T \leqslant 100$ °C, which is much less than the thickness illuminated by the electron beam (~ 10 nm). Second the positions occupied by the heavy cations which are easily identified in the HREM-image are in agreement with the data from an x-ray crystallographic analysis of the initial specimen. Moreover studies of crystals with an average oxygen concentration corresponding to $YBa_2Cu_3O_7$ and $YBa_2Cu_3O_{6.5}$ fabricated using the method noted above revealed a lack of specific lattice distortions and coincidence of the interplanar crystal spacing with those obtained from x-ray measurements in the former and doubling of the lattice parameter a characteristic of crystals with $x = 0.5$ (Ref. 19) in the latter. Both the internal regions of the specimen and those adjacent to the surface were analyzed.

These studies revealed that the structures of the specimens differed substantially in the bulk and near the surface. Figure 1, a, shows the characteristic structure of a bulk layer. In the (001) plane this structure consists of an array of blocks with transverse dimensions of 8–10 nm largely elongated in the [110] directions. The observed diffraction contrast is related to elastic distortions produced by these blocks. An analysis of the specimens in the (100) plane revealed that they are divided into layers of ~ 20 nm differentiated by the value of the parameter c, while the cation sublattice is identical in the various layers. Accounting for the information obtained from the images in the (001) plane we conclude that in the interior the crystal consists of parallelepiped blocks of $\sim 100 \times 10 \times 20$ nm^3. The two perpendicular orientations of these parallelepipeds in the (001) plane indicates that these directions are equivalent and, consequently, reveals a tetragonal host. Essentially two types of blocks are observed in the HREM-image (Fig. 1, b): Blocks with ordered chains of oxygen vacancies forming the (100) parallel planes and responsible for doubling of the unit cell
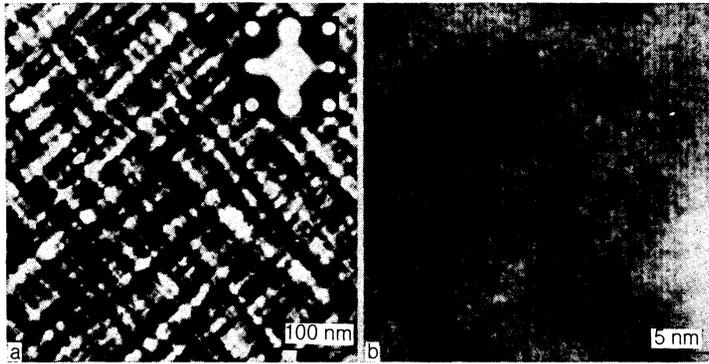
FIG. 1. Characteristic structure of the internal layer of the specimen: a — Microstructure; the electron diffraction pattern corresponding to this structure and shown in the insert has the axis of the [001] zone; b—HREM-image.

parameter a (Fig. 1, b, region A) and blocks without vacancy chains (Fig. 1, b, region B). According to Ref. 19 the oxygen concentration in the block with vacancy chains is near $x = 0.5$. Since the average concentration corresponds to $x = 0.7$ in the specimens under analysis, we conclude that $x \approx 1$ holds in blocks without vacancy chains. The characteristic dimensions are identical for blocks of different structure. Therefore a division of the crystal bulk into blocks of tetragonal and rhombic structures is observed. Diffuse scattering in the [110] direction about the reflexes is clearly distinguishable in the electron diffraction pattern (Fig. 1, a). Such diffuse scattering can be attributed to the fact that the level of rhombic distortion of the blocks in the crystal bulk varies continuously from 0 in the tetragonal blocks with $x \approx 1$ to a maximum in blocks with $x \approx 0.5$.

The HREM-images of various regions at various distances from the surface in the bulk of these specimens were essentially similar, indicating a homogeneous depthwise oxygen distribution averaged over a volume far exceeding the volume of the individual structural blocks ($\sim 2 \cdot 10^{-14}$ mm^3), with the exception of the surface regions which will be discussed below. Such a uniform average oxygen distribution throughout the crystal differs from the previously-observed[21,22] significant variation in oxygen concentration on the c axis. It evidently results because the oxygen concentration and distribution in the bulk of crystals investigated in the present study, which have cooled from $T_q \sim 900$ °C, correspond to the equilibrium values at $T = T_q$, while there is a rather uniform oxygen distribution at such a high temperature. Naturally the crystal surface layers are enriched with oxygen during the cooling in air, while the thickness of the

enriched layer will be determined by the cooling rate of the specimen.

Two types of regions are observed in the layers adjacent to the crystal surface. The first type consists of two forms of alternating interlayers of 18–20 nm and 40–48 nm in thickness elongated along the (110) plane (Fig. 2, a). The width of the interlayer boundaries estimated from the HREM-image and the size of the bar in the electron diffraction pattern (Fig. 2, a) is 7–9 nm. Reflex splitting is clearly visible in the electron diffraction pattern, indicating the presence of sections with two characteristic rhombic distortion levels. It is possible to estimate the average oxygen concentration in the $2 \times 2 \, \mu\text{m}^2$ region from which the electron diffraction pattern is taken based on the magnitude of splitting of the maximum in the electron diffraction pattern and the dependence of the unit cell parameters on x (Ref. 1); this concentration was $x \approx 0.35$.

The HREM-image of this region (Fig. 2, b) shows the interlayers on both sides of the boundary. Ordered vacancy chains which cause the parameter a to double and produce diffusion maxima in the electron diffraction pattern (Fig. 2, a) are to the right of the interlayer boundary (region B, Fig. 2, b). As noted above, in this interlayer we have $x \approx 0.5$. There are no vacancy chains in the interlayer to the left of the boundary (region A, Fig. 2, b) indicating a high oxygen concentration near $x = 0$. Such an oxygen distribution is consistent with the estimate of the average $x \approx 0.35$ given above.

The second type of region in the surface layer of the crystal (Fig. 3) is a layer intermediate between the surface regions of the first type and those observed throughout the interior of the specimen. Sharper (2–4 nm) boundaries
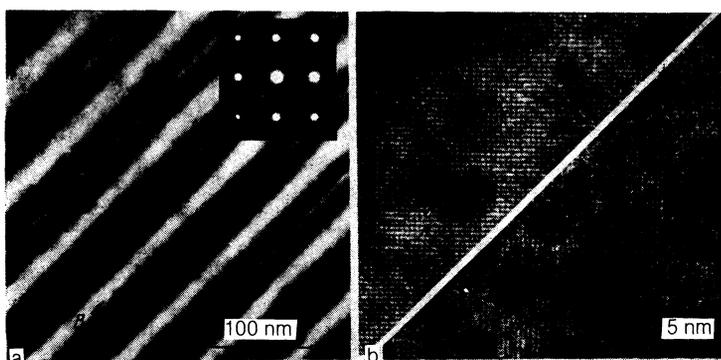

FIG. 2. First type of surface layer structure: a—Microstructure, its corresponding electron diffraction pattern in the insert has the axis of the [001] zone; A and B: Twinned interlayers of different cross-sections; b—HREM-images of twinned interlayers A and B.
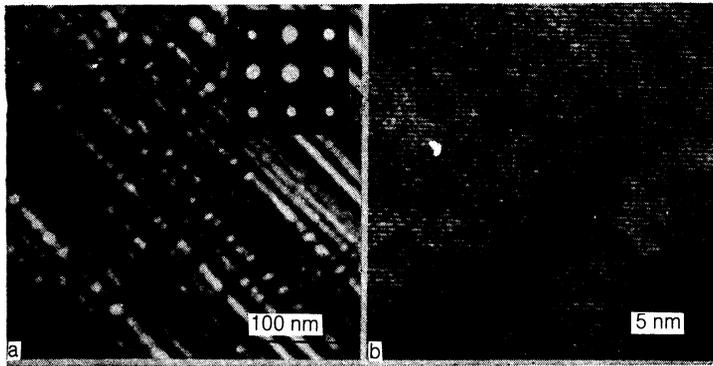
FIG. 3. Second type of surface layer structure: a—Microstructure; the electron diffraction pattern corresponding to this structure as shown in the insert has the axis of the [001] zone; b—HREM-image.

between the different sections compared to those observed in the bulk are characteristic of these regions, as is a change in the rhombic distortion level and, consequently, variation in oxygen concentration in isolated regions over a significant range, indicating weak diffuse scattering in the electron diffraction patterns in the [110] directions.

Results from structural analyses of the near-surface layers are in agreement with data from optical observations of specimens in reflected polarized light. The surface of the specimens etched from both sides, i.e., an area in the interior of the initial specimens, is optically isotropic. Obviously this is related to the period of the blocks of tetragonal and rhombic symmetry that is unresolvable in the optical range (a period of 8–10 nm); the overall packing of these blocks (Fig. 1, a) suggests a pseudotetragonal optical symmetry. The surface of the initial specimens (prior to annealing and after growing) is divided into regions whose quenching differential (Fig. 4) indicates their biaxiality[28] as well as a change in the position of axes a and b in the transition through the [110] boundary between the macroregions. It follows from a comparison to the HREM images (Fig. 2, a) that the a and b axes discussed above should be classified as domains with the predominant period lying in the alternation of the interlayers (18–20 nm and 40–48 nm).

We know[29] that annealing of sufficient duration in a helium atmosphere at $T \leqslant 400$ °C will cause the superconductivity observed in $YBa_2Cu_3O_{7-x}$ crystals for $x > 0.5$ to vanish entirely while the corresponding change in the average x in the specimen is less than 0.01. In order to establish whether or not this inhomogeneity in oxygen distribution throughout the specimen is eliminated some of the test crystals were annealed in air at $T = 370$ °C for 64 hours and were then slowly cooled.

Figure 5 shows the temperature dependence of the change in frequency of an LC-oscillator caused by inserting the test specimen into its inductance coil. The initial specimen, an annealed specimen and an initial specimen with the surface layers removed by ion etching to a depth of ~ 1 μm were tested. The results are explained assuming that the superconductivity of the initial crystal is determined by an oxygen-saturated surface layer $\leqslant 1$ μm thick. This explanation is consistent with the structural data given above and the assumption that during annealing in air, oxygen diffuses from the surface into the crystal bulk. It is significant that the distance over which the oxygen ions are to diffuse in this case is less than their characteristic diffusion length in the annealing process outlined above. This length can be estimated from known quantities: The diffusion coefficient is $D = 5 \cdot 10^{-8}$ cm$^2 \cdot$s^{-1} at $T = 550$ °C and the heat of solution of oxygen is $J = 180$ kJ$\cdot$mol.$^{-1}$ (Ref. 30). Repeat annealing of this type in an oxygen atmosphere, as we see from Fig. 5, will restore the superconducting properties of the surface.

Ionic etching did not alter the bulk properties of the crystal, since the temperature and width of superconducting transition in the control crystal with $x = 0$ remained unchanged after surface etching ($T_c = 92.5$ K; $\Delta T_c = 0.5$ K). We note that special measurements on specimens with $x = 0$ did not confirm the data reported in Ref. 31 indicating a change in the parameter c over time at room temperature.

After this crystal annealing, accompanied by oxygen diffusion over a distance greater than the characteristic dimensions of the structural blocks (~ 10–20 nm), the structure of the internal layers remained unchanged. It then follows that the irregular oxygen distribution throughout the specimen is a property characteristic of the $YBa_2Cu_3O_{7-x}$ compound with a low oxygen concentration ($x > 0.5$). The
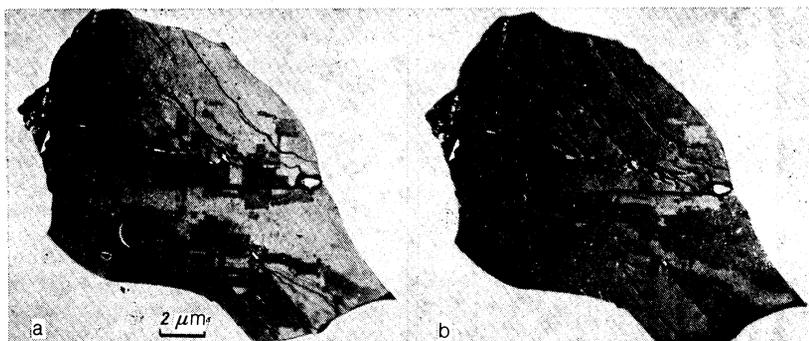

FIG. 4. Overall view of the macroscopic twinning configurations characteristic of the test single crystals; reflected polarized light; "a" and "b" are inverted by $\sim 5°$ with respect to the quenching position common to the macroscopic twins.
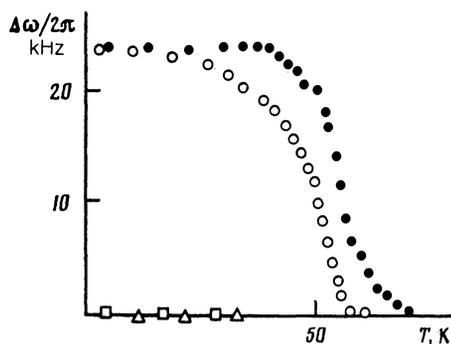
FIG. 5. Temperature dependence of the frequency shift of an LC-oscillator: O — initial specimen; ● — initial specimen minus surface layers and subsequently annealed in oxygen; □ and △ — initial specimen with surface layers etched down to $\sim 1\,\mu$m and the initial specimen annealed in air, respectively.

crystal divides spontaneously into clusters with different oxygen concentrations.

The observed irregularity of oxygen distribution in all likelihood is determined by a certain effective interaction between the vacancies which causes the division into clusters to become energy efficient[18,32] although evidently this distribution may also be affected by the crystal defects. The possibility of oxygen cluster formation has been noted previously; specifically in calculating the structure of $YBa_2Cu_3O_{7-x}$ with a random x (Ref. 16). According to Ref. 16 with a random x the crystal will divide into clusters with a certain set of values of x ($x = 1 - 2/n$ and $x = 1/n$, where $n \geqslant 2$ is an integer). The issue of oxygen clusters several lattice constants in size was also considered in Ref. 18 in discussing one possible $YBa_2Cu_3O_{7-x}$ structure with $x > 0.5$ when the crystal divides into microscopic orthorhombic blocks inverted with respect to one another, while consistent with x-ray structural analyses the crystal has a tetragonal structure. Reference 18 also proposed one possible cause of the mutual attraction of oxygen vacancies: The number of Cu^+ cations having the atypical number of three nearest O^{2-} anions diminishes with diminishing distance between the vacancies.

The results are in complete agreement with the x-ray crystallographic analysis data from Ref. 20 for unannealed crystals. However, the conclusion in Ref. 20 that the specimen contains only two types of structural blocks with $x = 1$ and $x = 0.5$ is not confirmed by our data, which indicate a continuous variation in the local values of x over the range from ≈ 0.5 to ≈ 1.

In conclusion we note that in interpreting the physical properties of $YBa_2Cu_3O_{7-x}$ compounds with $x \geqslant 0.5$ it is necessary to account for the possibly significant nonuniformity of its oxygen composition. Specifically the singularity on the $T_c(x)$ trace as well as the variation in conductivity near $x = 0.5$ may not be due to the correlation effects in the electron subsystem[29] but rather to percolation phenomena.

In interpreting the results of analyses of the electrical properties of $YBa_2Cu_3O_{7-x}$ superconductors it is also important to account for the possibility of noticeable oxygen overenrichment of the surface layers. On the other hand the possibility of fabricating a sufficiently thin surface layer with a high oxygen concentration may be promising for developing quasi-two-dimensional superconducting structures based on single crystals.

[1] R. J. Cava, B. Batlogg, C. H. Chen et al., Phys. Rev. **B36**, 5719 (1987).

[2] E. Takayama-Muromachi, Y. Uchida, M. Ishii et al., Jap. J. Appl. Phys. **26**, L1156 (1987).

[3] K. Kishio, J. Shimoyama, T. Hasegawa et al., Jap. J. Appl. Phys. **26**, L1228 (1987).

[4] J. D. Jorgensen, B. W. Veal, W. K. Kwok et al., Phys. Rev. **B36**, 5731 (1987).

[5] P. P. Freitas and T. S. Plaskett, Phys. Rev. **B36**, 5723 (1987).

[6] M. Tokumoto, H. Ihara, T. Matsubara et al., Jap. J. Appl. Phys. **26**, L1565 (1987).

[7] Y. Kubo, Y. Nakabayashi, J. Tabuchi et al., Jap. J. Appl. Phys. **26**, L1888 (1987).

[8] N. G. Stoffel, J. M. Tarascon, Y. Chang et al., Phys. Rev. **B36**, 3986 (1987).

[9] Y. Yguchi, A. Sugushita, M. Yanagisawa et al., Jap. J. Appl. Phys. **27**, L992 (1988).

[10] H. Verweij and W. H. M. Bruggink, J. Phys. Chem. Sol. **50**, 75 (1989).

[11] D. O. Welch, V. J. Emery and D. E. Cos, Nature, **327**, 278 (1987).

[12] Y. Matsui, E. Takayama-Muromachi, A. Ono et al., Jap. J. Appl. Phys. **26**, L777 (1987).

[13] Y. Matsui, Jap. J. Appl. Phys. **26**, L2021 (1987).

[14] K. Hiraga, D. Shindo, M. Hirabayashi et al., J. Electron. Microsc. **30**, 261 (1987).

[15] K. Nakamura and K. Ogawa, Jap. J. Appl. Phys. **27**, L577 1988).

[16] A. A. Aligia, A. G. Rojo and B. R. Alascio, Phys. Rev. **B38**, 6604 (1988).

[17] H. Verweij, Sol. St. Comm. **67**, 109 (1988).

[18] J. L. Hodeau, P. Bordet, J. J. Capponi et al., Physica C **153–155**, 582 (1988).

[19] H. W. Zandbergen and G. Thomas, Phys. Stat. Sol. (A) **107**, 825 (1988).

[20] V. N. Molchanov, L. A. Muradyan and V. I. Simonov, Pis'ma v ZhEhTF **49**, 222 (1989) [JETP Lett. **49**, 257 (1989)].

[21] M. Couach, A. F. Khoder, B. Barbara et al., Physica C **153–155**, 844 (1988).

[22] B. Ya. Kotyuzhanskiy and L. E. Svistov, Pis'ma v ZhEhTF **47**, 317 (1988) [JETP Lett. **47**, 381 (1988)].

[23] J. A. Mydosh, J. Phys. B **68**, 1 (1987).

[24] H. Sawada, T. Iwazumi, Y. Saito et al., Jap. J. Appl. Phys. **26**, L1054 (1987).

[25] P. Monod, M. Ribault, F. D'Yvoire et al., J. Phys. (France) **48**, 1369 (1987).

[26] Z. Z. Wang, J. Clayhold, N. P. Ong et al., Phys. Rev. B **36**, 7222 (1987).

[27] A. B. Bykov, L. N. Demianets, I. P. Zibrov et al., J. Cryst. Growth, **91**, 302 (1988).

[28] H. Schmid, J. P. Rivers, M. Clin et al., Physica C **153–155**, 1748 (1988).

[29] I. V. Aleksandrov, A. P. Volodin, I. N. Makarenko et al., Pis'ma v ZhEhTF, **49**, 287 (1989) [JETP Lett. **49**, 327 (1989)].

[30] J. M. O'Sullivan and B. P. Chang, Appl. Phys. Lett. **52**, 1441 (1988).

[31] I. V. Aleksandrov, A. B. Bykov, I. P. Zibrov et al., Pis'ma v ZhEhTF **48**, 449 (1988) [JETP Lett. **48**, 493 (1988)].

[32] W. R. McKinnon, M. L. Post, L. S. Selwyn and G. Pleizier, Phys. Rev. **B38**, 6543 (1988).

Translated by Kevin S. Hendzel